Iron and Uroporphyrin in Hepatocytes of Inbred Mice in Experimental Porphyria: A Biochemical and Morphological Study

PETER D. SIERSEMA,[1] RENÉ P. VAN HELVOIRT,[2] DIANE A.M. KETELAARS,[3] MAUD I. CLETON,[2] WIM C. DE BRUIJN,[3] J.H. PAUL WILSON[1] AND HENK G. VAN EIJK[2]

[1]*Department of Internal Medicine, University Hospital Rotterdam-Dijkzigt, 3015GD Rotterdam, and Departments of* [2]*Chemical Pathology and* [3]*Pathology, Erasmus University Rotterdam, 3015GE Rotterdam, The Netherlands*

Hexachlorobenzene-induced porphyria is iron dependent and characterized by the decreased activity of uroporphyrinogen decarboxylase and the accumulation of porphyrins in the liver. To examine the relationship between iron and porphyrins in liver tissue, we performed a biochemical and morphological (histological, ultrastructural and morphometrical) study in the livers of C57BL/10 mice. Mice were treated with hexachlorobenzene, iron dextran or the combination of hexachlorobenzene and iron dextran. An accumulation of porphyrins and an increased total iron content were found not only in the livers of mice treated with hexachlorobenzene and iron dextran but also in mice treated with iron dextran alone. In contrast, the amount of porphyrins was only slightly increased in the livers of mice treated with hexachlorobenzene alone. Needle-like structures, representing uroporphyrin crystals, were observed, histologically and ultrastructurally, in hepatocytes of mice treated with hexachlorobenzene and iron dextran and with iron dextran alone. Uroporphyrin crystals and ferritin iron were found in the same hepatocyte. A single uroporphyrin crystal, surrounded by ferritin iron, was observed in a hepatocyte of a mouse treated with hexachlorobenzene alone. Both in the livers of mice treated with hexachlorobenzene and iron dextran and in the livers of mice treated with iron dextran alone, morphometrical analysis showed that an increased area fraction of uroporphyrin crystals was associated with an increased area fraction of ferritin iron in hepatocytes.

Conclusions: In C57BL/10 mice, experimental porphyria can be induced by iron overload alone; uroporphyrin crystals and ferritin iron are located in the same hepatocyte; and the morphological cooccurrence of uroporphyrin crystals and ferritin iron in hepatocytes suggests a role for iron (as ferritin) in the pathogenesis of porphyria. (HEPATOLOGY 1991;14: 1179-1188.)

Several polyhalogenated aromatic hydrocarbons (PAHs), including hexachlorobenzene (HCB), produce in humans and animals a form of hepatic porphyria closely resembling human porphyria cutanea tarda (PCT). Both PCT and experimental porphyria are characterized by the decreased activity of uroporphyrinogen decarboxylase (URO-D; EC 4.1.1.37) and by the accumulation of uroporphyrins and heptacarboxylporphyrins in the liver (1-3).

The exact mechanism of HCB-induced porphyria is not clear. It has been demonstrated that the administration of HCB or other PAHs causes the induction of a particular isoenzyme of cytochrome P-450, cytochrome P-450Ia2 (4, 5). No evidence exists that HCB is converted by a cytochrome P-450–dependent reaction to metabolites that inhibit URO-D (6, 7). Because PAHs, including HCB, are poor substrates for the cytochrome P-450 isoenzyme, recently favored theories suggest that the induction of cytochrome P-450Ia2 by HCB could lead to the uncoupling of the microsomal system. Subsequently, reactive oxygen species could be produced (5, 8-14) that, under certain circumstances, initiate the formation of an inhibitor of URO-D (12, 14-16) and/or oxidize uroporphyrinogen to uroporphyrin (11, 13). Because uroporphyrin is not a substrate for URO-D, accumulation results (17). As in human PCT, iron is important in HCB-induced porphyria (1, 9, 18-25). If, as a result of cytochrome p-450 induction, reactive oxygen species such as the superoxide radical are produced and "free" iron is present, the highly reactive hydroxyl radical ($OH^{\cdot}$) could be formed by way of the Haber-Weiss reaction (26). In the presence of the hydroxyl radical a variety of reactions could be initiated (27, 28).

In PCT, histological and ultrastructural (light microscopy [LM] and electron microscopy [EM]) studies revealed needle-like structures, representing uroporphyrin crystals, in hepatocytes (29-37). In addition, in HCB-induced porphyria research four morphological studies have been published (38-41), of which only one study reported the presence of needle-like structures in hepatocytes (39). In PCT and in experimental porphyria the nature of the endogeneous iron pool involved and its correlation with the site within the liver where uropor-

Received October 22, 1990; accepted July 12, 1991.

Adress reprint requests to: Peter D. Siersema, M.D., Department of Internal Medicine, University Hospital Rotterdam-Dijkzigt, Dr. Molewaterplein 40, 3015 GD Rotterdam, The Netherlands.

31/1/32844

phyrin production takes place are not clear. In PCT, one LM study investigated the histological relationship between porphyrins and iron, reporting that no correlation was seen between areas of porphyrin fluorescence and areas of stainable iron (42). Regarding HCB-induced porphyria, no study on the morphological relationship between porphyrins and iron has been published. We therefore performed a biochemical, histological, ultrastructural (both LM and EM) and morphometrical study on livers of C57BL/10 mice that were treated with HCB, iron dextran as Imferon (IMF) or the combination of HCB and IMF.

MATERIALS AND METHODS

Chemicals. HCB was purchased from Merck AG (Darmstadt, Germany) ferrihydroxide-dextrane (Imferon) was purchased from Fisons Pharmaceuticals (Vleusden, The Netherlands) and Avertin was purchased from Aldrich-Chemie GmBH & Co. (Steinheim, Germany). All other chemicals were of the highest purity commercially available.

Animals and Treatment. This study was performed according to the "Regulations for use of laboratory animals in the Erasmus University Rotterdam" laid down by the Laboratory Animal Committee of the Erasmus University. Male C57BL/10 mice, weighing 20 to 25 gm, were purchased from the Centraal Proefdier Bedrijf (Zeist, The Netherlands). The mice were divided into five groups: groups 1 to 3 consisted of 10 mice each, and groups 4 and 5 consisted of 4 mice each. Mice in group 1 were treated with 16 mg of HCB in two doses of 8 mg. HCB dissolved in 0.4 ml warm corn oil was injected intraperitoneally. Mice in group 2 were treated with IMF, 12 mg/mouse, also injected intraperitoneally. Mice in group 3 were treated with the combination of HCB (16 mg/mouse) and IMF (12 mg/mouse) intraperitoneally. HCB was given in two doses of 8 mg, on day 1 and day 4, and IMF was given on day 1. Mice in group 4 received only 0.4 ml warm corn oil intraperitoneally on day 1 and day 4, and mice in group 5 were not treated.

Urine from the mice was collected once a week for the determination of porphyrin excretion. For this purpose mice were housed for 24 hr in metabolic cages. Urinary porphyrin excretion increased after 3 wk in group 3 and after 9 wk in group 2. After 26 wk urinary porphyrin excretion remained almost undetectable in groups 1, 4 and 5. Uroporphyrin excretion was maximal in group 3 after 14 wk. From 14 wks up to 26 wk, uroporphyrin excretion remained at the same level in group 3. In group 2, uroporphyrin excretion increased more slowly; however, it was still increasing after 26 wk. Therefore we decided to do the observations for this study at 18 wk.

Under anesthesia with Avertin, two liver lobes were removed for the measurement of total porphyrin content, hepatic URO-D activity and total iron content in four livers of mice in groups 1 to 3 and of two mice in groups 4 and 5. For the LM and EM study of the remainder of the liver, the portal vein was cannulated, and the liver was perfused with 3% glutaraldehyde in 0.14 mol/L cacodylate buffer, pH = 7.4 (275 mOsm), at 37° C. Frozen sections were prepared from the livers of two mice in groups 1 to 3. For this purpose unperfused livers were removed from anesthesized mice and immediately frozen in liquid nitrogen.

Measurement of Porphyrins. For the measurement of porphyrins in the livers, the lobes were homogenized to yield a 10% homogenate in Tris-HCl buffer (50 mmol/L, pH = 8.0), which was centrifuged for 10 min at 1,800 *g*. After freeze-drying and methylation the porphyrins in liver tissue were measured by high-pressure liquid chromatography as described earlier (43). Protein was measured according to Lowry et al. (44). The amount of porphyrins was expressed in picomoles per milligram of protein.

URO-D activity. URO-D activity was assayed in supernatant fractions of homogenates of liver tissue as previously described by Francis and Smith (45), using pentacarboxylporphyrinogen I as substrate. Protein was measured according to Lowry et al. (44). URO-D activity was expressed as the amount of coproporphyrinogen I formed in picomoles per minute per milligram of protein.

Total Liver Iron Content. Total liver iron content was determined using a modification of the method described by Harris (46). Homogenized liver tissue was dried at 110° C overnight. The amount of liver tissue was weighed with an accuracy of 0.01 mg. To the dried tissue, 0.2 ml perchloric acid (70% wt/vol) was added, and this was heated. After cooling, distilled water was added until a volume of 2.0 ml was reached. From this solution 0.2 ml was taken, and 0.1 ml HCl (1 mol/L), 0.2 ml ascorbic acid (25 gm/L), 0.1 ml sodium acetate (saturated) and 0.2 ml Ferrozine (Sigma Chemical Co., St. Louis, MO) were added. This solution was vigorously mixed. After 10 min the extinction was measured at 562 nm against four standard iron solutions of 20, 50, 150 and 300 μmol/L each. Each of the standards was made separately. The amount of liver iron was expressed as mmol/100 gm dry wt.

LM and EM Study. For LM, a part of the fixed liver was dehydrated briefly through graded alcohol series, embedded in paraffin, serially sectioned and stained. The staining protocol included Gill's hematoxylin stain (with reduced water contact) (32), the ferric ferricyanide reduction test in Lillie's modification and Perls' Prussian blue stain for ferric iron (47). Histological results, birefringence and fluorescence (excitation filter with a transmission range of 300 to 420 nm and an absorption filter with a transmission peak above 610 nm) were studied with a Zeiss axioplan microscope (Carl Zeiss, Oberkochen, Germany).

Because uroporphyrins have been described to be water soluble (29, 32), two procedures were used for EM. First, small blocks were taken randomly from the fixed livers, dehydrated briefly through graded acetone series and embedded in Epon (direct method). Second, paraffin-embedded liver blocks, in which needle-like structures were found with LM, were deparaffined with xylol, followed by immersing in acetone and embedding in Epon (indirect method). Ultrastructurally, no essential differences were seen between liver tissue processed according to either the direct or the indirect method (results not shown). Ultrathin sections (60 nm) were collected on copper grids and examined with and without conventional staining (uranyl acetate and lead citrate) in a Zeiss EM 902 transmission microscope (Carl Zeiss). This instrument is equipped with an integrated electron spectrometer allowing high-resolution imaging with energy-filtered electrons (i.e., electron spectroscopic imaging [ESI]). For technical details see Sorber et al. (48, 49).

Morphometrical Procedure. To determine the area fraction (expressed as a percentage of the measured cytoplasmic frame area) of uroporphyrin crystals and ferritin-iron core particles, the image analyzer IBAS 2000 (Kontron/Zeiss, Munich, Germany) was used. Grey-value frequency histograms were used for objective segmentation and discrimination between ferritin and uroporphyrin crystals. For technical details see Sorber et al. (48, 49) and Cleton et al. (50). Unstained Epon sections, 500 to 750 nm thick, were visualized by reflection contrast microscopy with the use of a Zeiss antiflex plan-

TABLE 1. Biochemical data of liver tissue in different groups of mice after 18 wk

Treatment group	n	Porphyrin content[a]		URO-D activity[b]	Iron content[c]
		URO	C7[c]		
1. HCB	4	2.0 ± 0.4	–	36.4 ± 1.4	0.5 ± 0.2
2. IMF	4	150 ± 38[d]	17 ± 3.1[e]	3.2 ± 1.0[d]	10.1 ± 0.8[d]
3. HCB and IMF	4	439 ± 43[d]	49 ± 5.8[d]	2.6 ± 0.9[d]	9.9 ± 0.7[d]
4. Corn oil	2	–	–	39.1 ± 1.2	0.4 ± 0.2
5. Control	2	–	–	39.8 ± 1.4	0.4 ± 0.2

URO = uroporphyrin; C7 = heptacarboxylporphyrin; – = not increased.
[a]Mean (± S.D.) in picomoles per milligram protein.
[b]Mean (± S.D.) in picomoles per minute per milligram protein.
[c]Mean (± S.D.) in mmol/100 gm dry weight.
[d]$p < 0.001$.
[e]$p < 0.005$.

neofluar, 63x/1.25, Ph3, oil-immersion objective (51, 52). Images were transfered to the IBAS with a sensitive camera mounted on the Zeiss axioplan. Because only a single uroporphyrin crystal and nearly no ferritin iron were detected in the livers of mice treated with HCB alone, only the livers of mice treated with the HCB and IMF combination and the livers of mice treated with IMF alone were measured. In liver sections from each treatment group, 40 cytoplasmic areas of 8,100 μm^2 were randomly selected and measured for both the area fraction of uroporphyrin crystals and the area fraction of ferritin iron present in each area.

Statistics. Total porphyrin content, indirect URO-D activity and total iron content in the livers of the various groups were tested for significant differences using the Wilcoxon's rank sum test.

RESULTS

Biochemistry. Results of mean ± S.D. liver porphyrin content, mean (±S.D.) hepatic URO-D activity and mean (±S.D.) total liver iron content in the different groups of mice at 18 wk are given in Table 1. In group 3 and to a lesser extent in group 2, hepatic uroporphyrins and heptacarboxylporphyrins were significantly increased compared with group 5. No significant increase of liver porphyrins in groups 1 and 4 was seen. URO-D activity was significantly decreased in groups 2 and 3 but not in groups 1, 4 and 5. Total liver iron was significantly increased in mice treated with IMF (groups 2 and 3). To exclude the possibility that different lobes had different porphyrin content, URO-D activity and iron content, we determined these parameters in different lobes of two livers of mice in groups 1, 2 and 3. No interlobar differences were found.

Morphological Observations. On macroscopic examination, the livers of mice treated with HCB (groups 1 and 3) were slightly enlarged compared with the livers of mice in groups 2, 4 and 5. The color of the livers of mice in group 1 was yellow, in group 2 it was dark brown and in group 3 it was yellowish brown compared with the normal color of the livers in the control groups (groups 4 and 5).

Light Microscopy. LM examination in all five groups did not show evidence of inflammatory infiltration, spotty necrosis or fibrosis. In groups 2 and 3 the nuclei of the hepatocytes appeared somewhat enlarged compared with the other groups, and some nuclei contained up to three nucleoli. This was more pronounced in group 3 than in group 2. In hepatocytes of mice treated with either HCB in corn oil (groups 1 and 3) or corn oil alone (group 4), an increased amount of fine lipid droplets with a patchy distribution was found in approximately 50% of the hepatocytes. In hepatocytes of mice in group 3 and to a lesser extent in group 2, needle-like structures were present (Fig. 1a), which displayed birefringence after examination with polarized light (Fig. 1b). In serially cut sections the ferric ferricyanide reduction test in Lillie's modification showed needle-like structures in group 3 and to a lesser extent in group 2 (Fig. 1c). With Perls' Prussian blue stain, an increased amount of ferric iron was found to be located diffusely throughout the liver in livers of mice in groups 2 and 3, both in hepatocytes and in Kuppfer cells (Fig. 1d). In contrast to the iron distribution, the needle-like structures were not regularly distributed but were found in relatively circumscribed areas in the liver, occupying about 50% of hepatocytes. Both needle-like structures and ferric iron were found to be located in the same hepatocyte (compare Fig. 1a-d).

We extended the study to examine whether needle-like structures also displayed fluorescence with UV light. When liver tissue of all five groups was examined with UV light, a diffuse autofluorescence was noticed that was caused by the use of glutaraldehyde fixation (47). Therefore frozen sections were used. In the livers of mice of groups 2 and 3, it was noticed that areas with needle-like structures (Fig. 2a) displayed fluorescence (Fig. 2b); however, fluorescence seemed more widespread and not limited to needle-like structures alone.

Comparison of LM with EM. Light microscopical and ultrastructural aspects of an unstained, ultrathin section containing a needle-like structure were compared in Figures 3a-c. With EM, the birefringent needle of Figure 3a appeared to be largely electron dense (Fig. 3b, c).

Electron Microscopy. In the livers of mice in which biochemically porphyrins accumulated (groups 2 and 3), in general only minor alterations in the ultrastructure of the hepatocytes were found. Comparing groups 1, 4 and 5, we observed that relatively more nuclei were hetero-

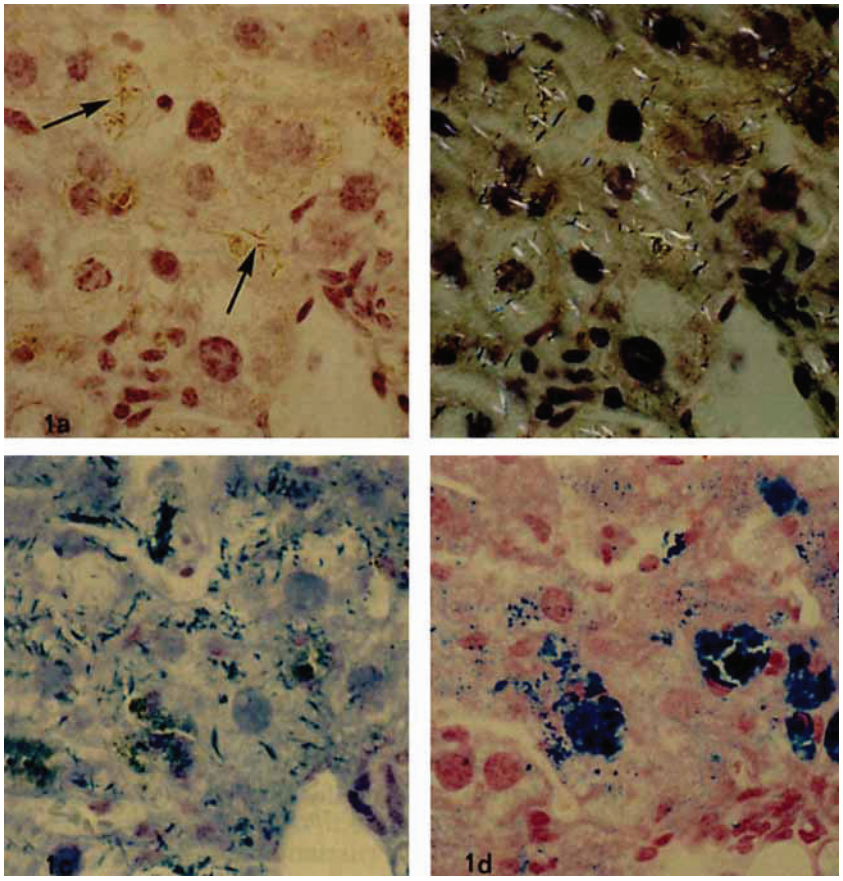

FIG. 1. Light micrographs (original magnification ×650) of the same field in four sequential sections of a liver from a mouse treated with hexachlorobenzene and iron dextran. (a) Gill's hematoxylin stain. Needle-like structures in hepatocytes display a brown color *(arrows)*. (b) Polarized light. Needle-like structures display birefringence. (c) Ferric ferricyanide reduction test in Lillie's modification. Needle-like structures in hepatocytes stain dark blue. (d) Perls' Prussian blue stain. Blue staining in hepatocytes and Kuppfer cells indicates the presence of ferric iron.

chromatic and that their contours were indented. Sometimes the intercellular area between adjacent hepatocytes was widened. In these areas, microvilli, formed by the lateral surfaces, were found to be projecting into the lumen (Fig. 4, *arrowheads*). In all four treatment groups the ultrastructure of bile canaliculi appeared to be affected; the lumen was enlarged with broadening or loss of microvilli (e.g., Figs. 4 and 5, *arrows*). Both the use of a large amount of corn oil (0.4 ml) and the iron preparation probably attributed to the alterations of the ultrastructure of bile canaliculi in groups 1 through 4. The ultrastructure of mitochondria and (rough and smooth) endoplasmic reticulum was similar in all five groups. In hepatocytes of mice treated with corn oil (groups 1, 3 and 4), an increased amount of lipid droplets was found (e.g., Fig. 5). Examination of unstained Epon sections showed needle-like stuctures in hepatocytes of mice of group 3 and to a relatively lesser extent in group 2. In group 1 only a single needle-like structure was observed. Needle-like structures were randomly located in the hepatocyte. In group 3, at low magnification numerous needle-like structures (Fig. 6a) were located in hepatocytes loaded with lipid droplets. Some occupied the same vacuole as the lipid (Fig. 6b), but others were found lying entirely or partly free in the cytoplasm (Fig. 6c). Iron in the cytoplasm of hepatocytes is best seen at higher magnification (Fig. 6c). It was found as hemosiderin/ferritin in siderosomes (iron-containing lysosomes) (Fig. 6a), as ferritin in vacuoles (Fig. 6a), sometimes as lipid-associated ferritin (Fig. 6b) and as cytoplasmic ferritin (Fig. 6c). Frequently, cytoplasmic ferritin formed aggregates called ferritin clusters (Fig. 6c). The iron nature of the ferritin particles in clusters and siderosomes could be unequivocally established with the Zeiss EM 902 electron spectrometer (results not shown) (53). Qualitatively, no significant differences were seen in the aspect of the needle-like structures and the iron distribution in hepatocytes between group 3 (Fig. 6 a-c) and group 2 (Fig. 7 a, b). The only difference between the two groups was the relative scarcity of lipid droplets in group 2. In hepatocytes of mice in group 1, very little ferritin iron was present. The needle-like structure, which was observed in these hepatocytes, was surrounded by ferritin (Fig. 8).

Morphometrical Analysis. The results of the morpho-

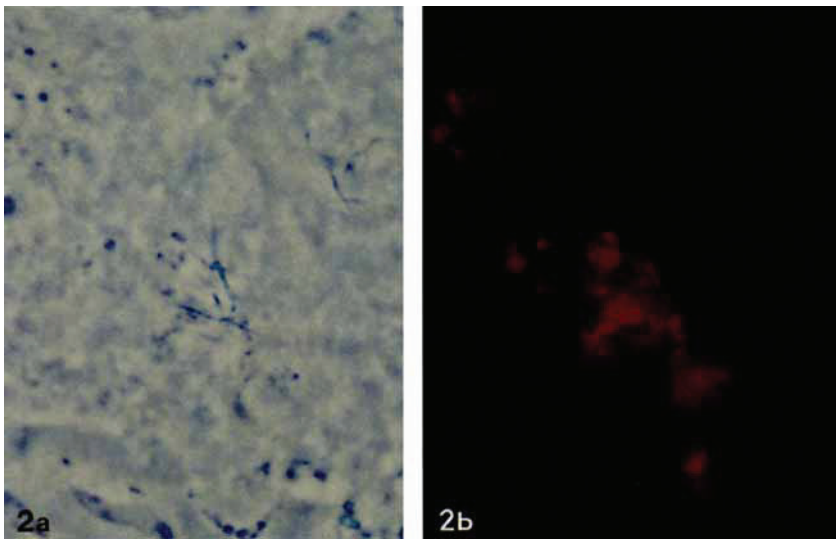

FIG. 2. (a) Light micrograph (original magnification ×1,000) (phase-contrast) of a frozen section of liver tissue of mouse treated with iron dextran, showing needle-like structures. (b) Light micrograph (original magnification ×1,000) of the same field, showing fluorescence in areas with the needle-like structures of Figure 2a. Note that fluorescence was more widespread and not limited to needle-like structures.

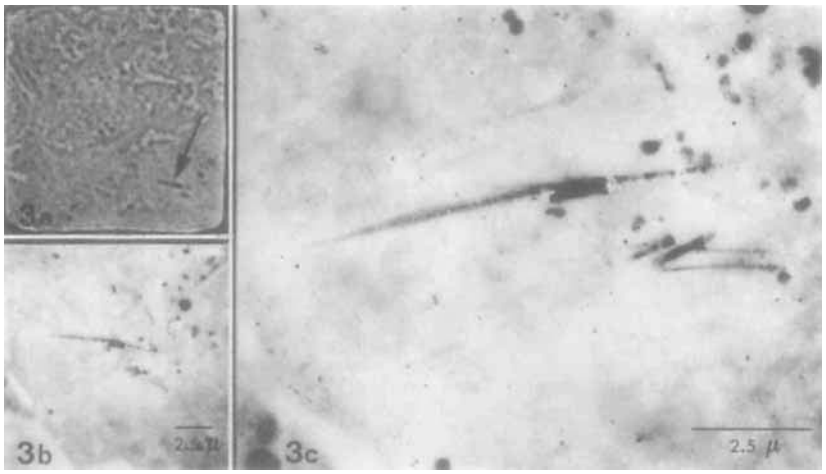

FIG. 3. Light micrograph of an ultrathin, unstained Epon section, mounted on a grid, of a mouse treated with hexachlorobenzene and iron dextran, demonstrating a needle-like structure *(arrow)* (original magnification ×500). (b) Electron micrograph of the same area showing the same needle-like structure (*bar* = 2.5 μm). (c) High-power electron micrograph of the same needle-like structure. Note the alternating areas of different electron density (*bar* = 2.5 μm).

metrical analysis in the livers of mice treated with HCB and IMF and in the livers of mice treated with IMF alone are given in Fig. 9a-b. As can be seen from this figure, an increased area fraction (expressed as a percentage of the measured cytoplasmic frame area) of uroporphyrin crystals present in each area was associated with an increased area fraction of ferritin iron. The difference between the two treatment groups was the increased area fraction of uroporphyrin crystals in the livers of mice treated with HCB and IMF compared with the livers of mice treated with IMF alone. However, the ratio between uroporphyrin crystals and ferritin iron was the same in both treatment groups (HCB and IMF: $Y = 0.41 + 2.02\ X$; IMF: $Y = 0.46 + 2.08\ X$).

DISCUSSION

A biochemically increased amount of hepatic porphyrins (Table 1) was found to coincide light microscopically with the presence of needle-like structures in liver parenchymal cells C57BL/10 mice (Figs. 1a-c, 3a). Electron microscopically, these needle-like structures appeared to be of alternating density (Fig. 3b, c). The needle-like structures represent uroporphyrin crystals because uroporphyrin I and III, crystallized *in vitro*, displayed the same ultrastructural characteristics (33). Uroporphyrin crystals were presumably synthesized *in vivo* in the liver because they were found in frozen sections (Fig. 2a). In areas where needle-like structures were found, fluorescence was also detected. The fluores-

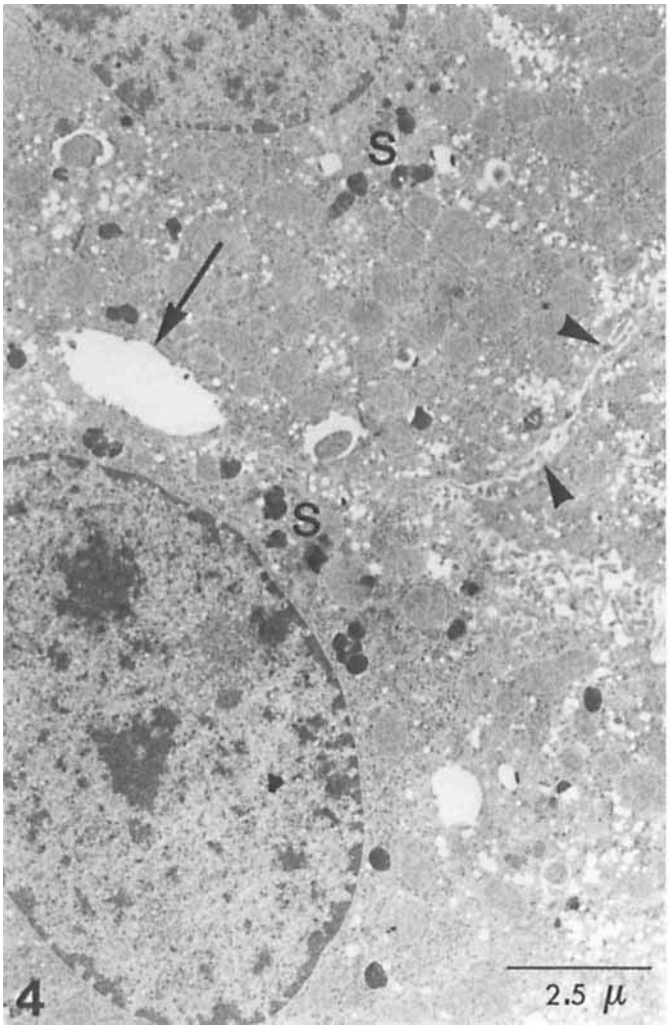

FIG. 4. Low-power electron micrograph (stained section) of hepatic parenchymal cells of a mouse treated with iron dextran. Note interdigitation of lateral cell membranes *(arrowheads)* and loss of microvilli in bile canaliculus *(arrow)*. Aspect of other cell organelles is normal. *S* = siderosome (iron-containing lysosome) (*bar* = 2.5 μm).

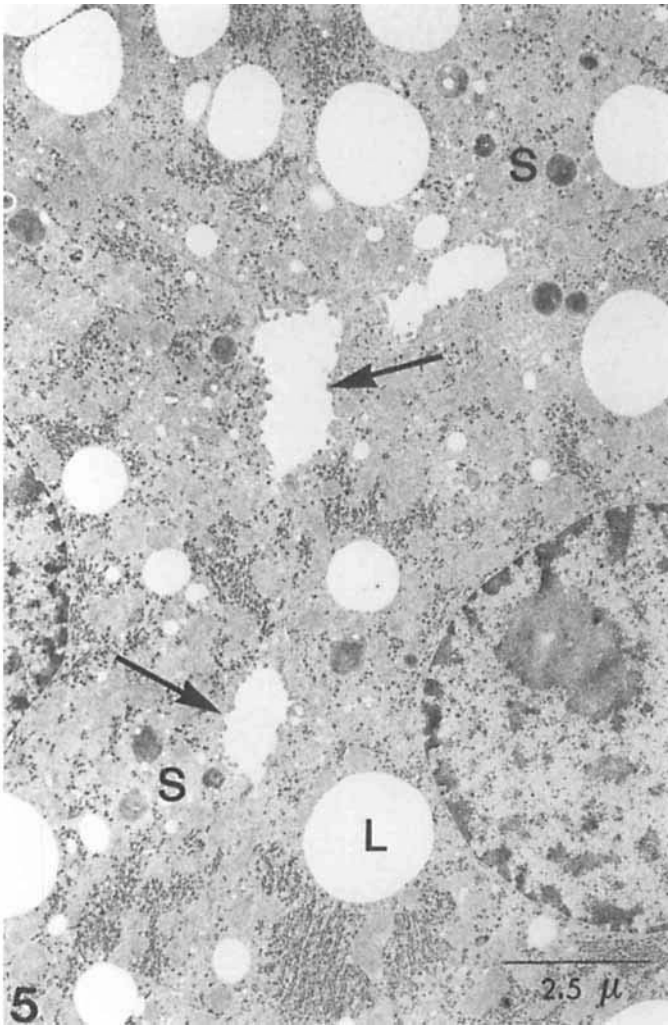

FIG. 5. Electron micrograph of hepatic parenchymal cells (stained section) of a mouse treated with hexachlorobenzene and iron dextran. Note abundance of lipid droplets and loss of microvilli in bile canaliculi *(arrows)*. Aspect of other cell organelles is normal. *S* = siderosome (iron-containing lysosome); *L* = lipid droplet (*bar* = 2.5 μm).

cence was not limited to uroporphyrin crystals but rather was more widespread in the surrounding cytoplasm (Fig. 2b). In accordance with an observation of Fakan and Chlumska (37), needle-like structures reduced ferric iron in the ferric ferricyanide reduction test, leading to a blue color in needle-like structures (Fig. 1c) (54). It seems unlikely that uroporphyrin crystals are responsible for the color reaction in the ferric ferricyanide reduction test because uroporphyrins are oxidized uroporphyrinogens. Whether the observed fluorescence (Fig. 2b) and the reducing substance responsible for the color reaction in the ferric ferricyanide reduction test (Fig. 1c) are the result of a mixture of (uro)porphyrinogens and (uro)porphyrins surrounding the uroporphyrin crystals remains to be established. Accumulation of uroporphyrins and heptacarboxylporphyrins and inhibition of URO-D were found not only in the livers of mice treated with HCB and IMF but also in mice treated with IMF alone. The only difference was that in the livers of mice treated with IMF alone the amount of porphyrins at 18 wk was less marked than in mice treated with HCB and IMF (Table 1). We were surprised to find that iron overload alone was capable of inducing porphyria in this strain of mice. Recently, this finding was also reported by Smith et al., (55) and Smith and De Matteis (56), using the same iron preparation. Iron dextran has been described as accumulating in hepatocytes as ferritin iron 3 to 4 wk after parenteral administration (57). Evidence on the role of HCB in experimental porphyria suggests that HCB induces cytochrome P-450Ia2 (4, 5), resulting in the production of oxidizing species (5, 8-14). The role of iron is explained by its ability to participate in free radical processes (26-28). Induction of the cytochrome P-450 system appears to depend on the binding of the chemical to a receptor protein (Ah phenotype) (4). Greig et al. (58)

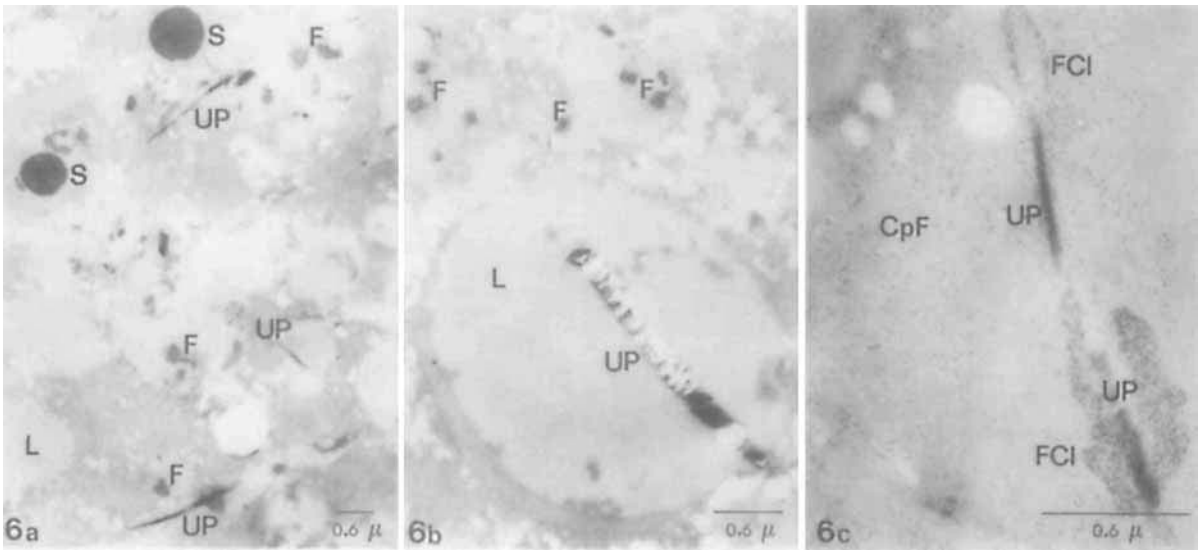

FIG. 6. Electron micrographs of a hepatic parenchymal cell (unstained section) of a mouse treated with hexachlorobenzene and iron dextran. (a) Note uroporphyrin crystals *(UP)* surrounded by siderosomes (iron-containing lysosomes, *S*) and lipid associated and/or vacuolar ferritin *(F)*. *L* = lipid droplet (*bar* = 0.6 μm). (b) Same section at higher magnification. Note association of uroporphyrin crystal *(UP)* and ferritin with lipid droplets (*bar* = 0.6 μm). (c) High-power electron micrograph of the same section, showing a uroporphyrin crystal *(UP)* surrounded by cytoplasmic ferritin clusters *(FCl)* and cytoplasmic ferritin *(CpF)* (*bar* = 0.6 μm).

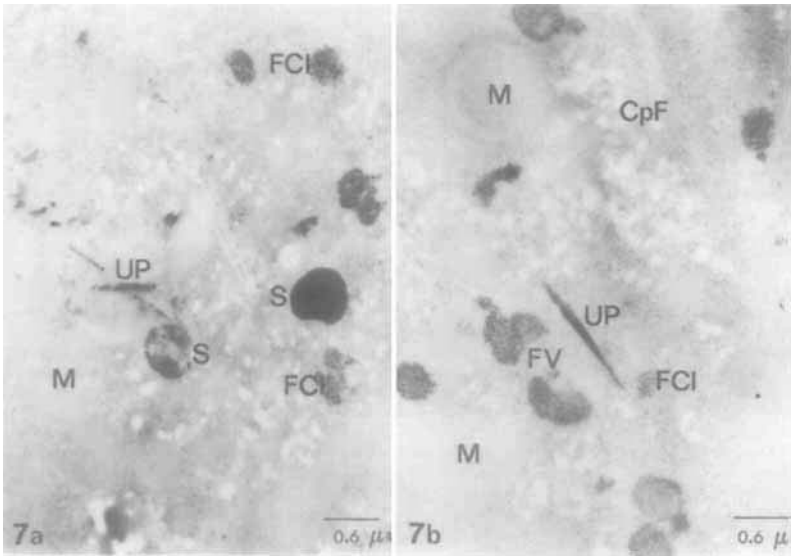

FIG. 7. Electron micrographs of a hepatic parenchymal cell (unstained section) of a mouse treated with iron dextran. (a) Note association of uroporphyrin crystal *(UP)* with a siderosome (iron containing lysosome, *S*). *FCl* = ferritin cluster; *M* mitochondrion (*bar* = 0.6 μm). (b) Same section. Note close association of uroporphyrin crystal with ferritin clusters *(FCl)* and ferritin containing vacuoles *(FV)*. *CpF* = cytoplasmic ferritin; *M* = mitochondrion (*bar* = 0.6 μm).

found that 2,3,7,8-tetrachlorodibenzo-p-dioxin, another PAH, induced porphyria both in C57BL/10 mice (Ah responsive) and in AKR mice (Ah nonresponsive). The 2,3,7,8-tetrachlorodibenzo-p-dioxin did not induce porphyria in DBA/2 mice (also Ah nonresponsive), even with concomitant iron administration. These results, and ours, suggest that the induction of the cytochrome P-450 system is not an absolute requirement for porphyria to develop. As a possible explanation for this observation, Cheeseman et al. (59) recently reported that NADPH/ADP iron-dependent lipid peroxidation in microsomes of C57BL/6 mice (Ah responsive) and AKR mice was increased twofold compared with microsomes of DBA/2 mice, suggesting that iron-catalyzed free radical–mediated processes are important in inducing porphyria. This difference in lipid peroxidation was also found in microsomes of C57BL/10 mice compared with microsomes of DBA/2 mice (55). The role of iron is

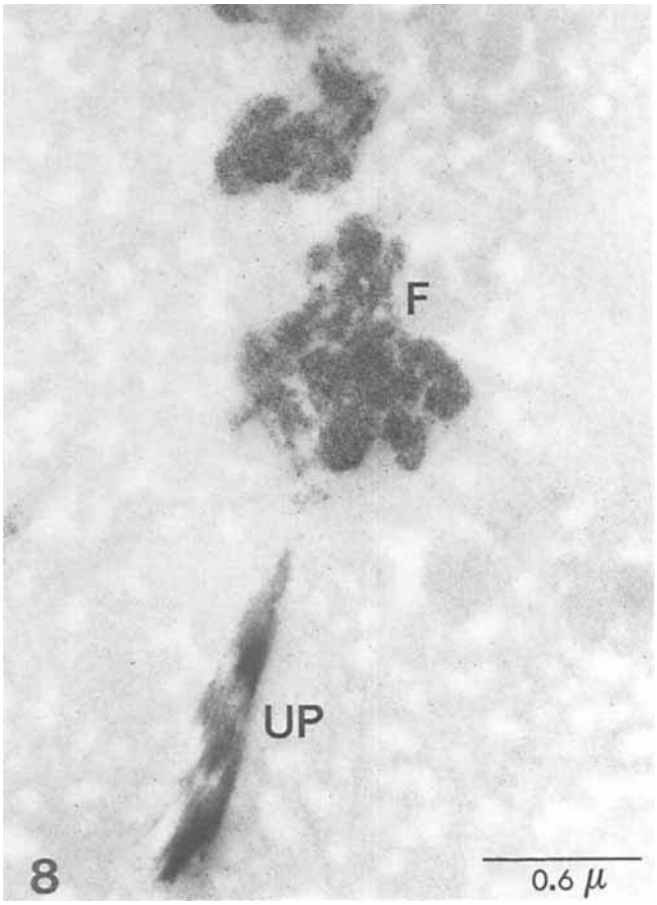

FIG. 8. Electron micrograph of a hepatic parenchymal cell (unstained section) of a mouse treated with hexachlorobenzene. Note association of uroporphyrin crystal *(UP)* with ferritin *(F)* (*bar* = 0.6 μm).

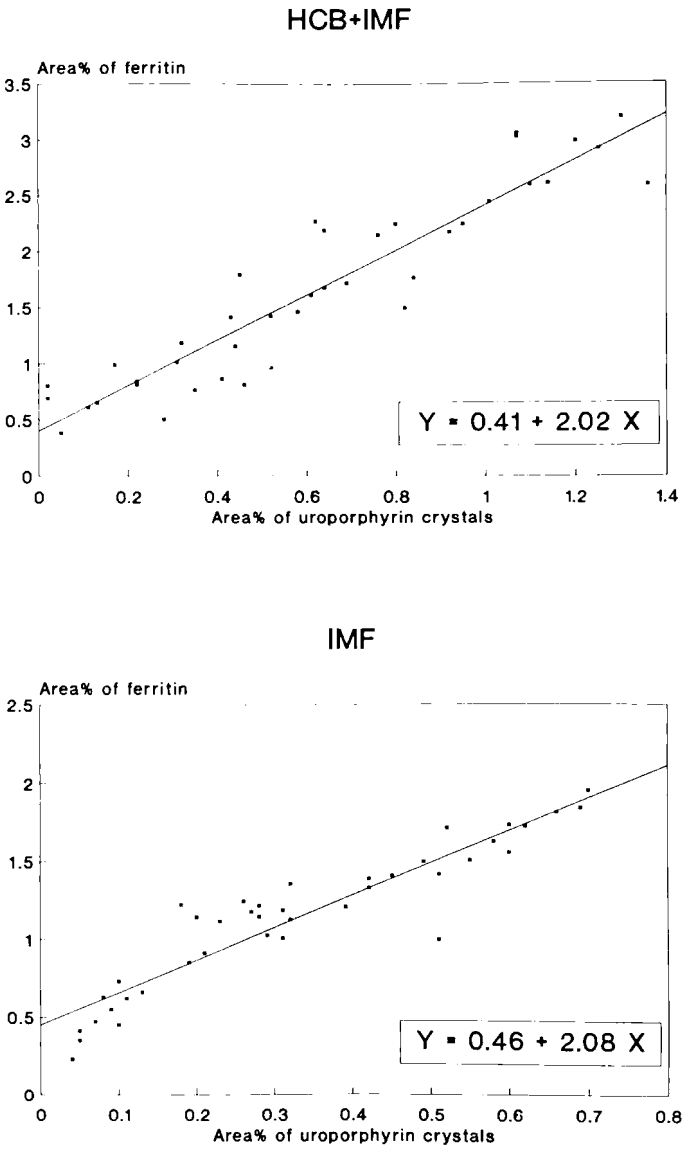

FIG. 9. Morphometrical analysis by reflection-contrast microscopy of unstained, thin Epon sections showing the linear relationship beteween area fractions of uroporphyrin crystals and area fractions of ferritin-iron cores. The area fractions are expressed as percentages *(%)* of the measured cytoplasmic frame area (40 areas of 8,100 μm^2). (a) Mice treated with the hexachlorobenzene and iron dextran *(HCB + IMF)*. (b) Mice treated with iron dextran *(IMF)* alone.

further illustrated by findings of Smith et al. (60), who described that the development of porphyria in rats treated with HCB alone depended on the endogenous iron content of the liver.

Petryka, Kostich and Dhar (42) were not able to demonstrate iron and porphyrin fluorescence in the same hepatocyte in PCT. They concluded that certain cells preferentially accumulate either porphyrins or iron. In contrast to their findings, we observed in hepatocytes of C57BL/10 mice that uroporphyrin crystals and ferritin iron were located in the same hepatocyte (Figs. 1, 6-8). Moreover, an increased area fraction of uroporphyrin crystals was associated with an increased area fraction of ferritin iron in each cytoplasmic area (Figs. 9a-b). The only difference was that at 18 wk the area fraction of both ferritin iron and uroporphyrin crystals in the livers of mice treated with IMF alone was reduced to about 50% of the values measured in the livers of mice treated with HCB and IMF. Nevertheless, the area fraction ratio was the same in the livers from both groups (Y = 0.5 + 2X). Additionally, the single uroporphyrin crystal found in a hepatocyte of a mouse treated with HCB alone was also surrounded by ferritin aggregates (Fig. 8), which was remarkable in light of the scarcity of (ferritin) iron present in these livers. Our results suggest a role for iron (as ferritin) in the pathogenesis of (experimental) porphyria. Reactive ferrous iron, however, is sequestered in ferritin as a nontoxic oxyhydroxide, complexed with phosphate (ferritin core = $[FeOOH]_8 \cdot [FeOOPO_3H_2]$); oxidation and the storage of ferrous iron appear to be related processes, and the release of iron from ferritin requires reduction (61). Although *in vitro* release of ferrous iron from ferritin by liver microsomes has been described (10, 18, 62, 63), it is not clear whether

this occurs *in vivo*. An intracellular pool of low molecular weight iron, acting as an intermediate stage between an increased availability of iron and ferritin, has been suggested by Jacobs (64). Moreover, evidence was found for a role of this pool in the radical formation in iron-loaded cells (65). Although attractive, definite evidence for the existence of a pool of low molecular weight iron has not been provided (66).

On the basis of our results we hypothesize that in hepatocytes of C57BL/10 mice a (genetically determined) active oxidative metabolism exists. Above a certain level of iron accumulation in hepatocytes (Fig. 9a-b), toxic species could be produced, which induces the formation of an inhibitor of URO-D (12, 14-16), the oxidation of uroporphyrinogen to uroporphyrin (11, 13) or both. A third possibility is direct damage of URO-D by way of a radical-mediated mechanism (67).

This study was conducted at 18 wks, at which time diffuse iron (as ferritin) and focal uroporphyrin accumulation still existed. Therefore a study is now in progress trying to establish the time-sequence relationship between uroporphyrin (crystal) formation and ferritin-iron accumulation.

Acknowledgments: We wish to thank Dr. F.W.J. ten Kate for assistance with the interpretation of the light microscopical slides; Mrs. R. Koole-Lesuis, Miss C.W.J. Sorber, Mr. J.B.H.J. van Lier, Mr. J. Slats and Mr. A.A.W. de Jong for expert technical assistance; and Miss P.C. Delfos for excellent photographic work.

REFERENCES

1. Sweeney GD. Porphyria cutanea tarda, or the uroporphyrinogen decarboxylase deficiency diseases. Clin Biochem 1986;19:3-15.
2. Marks GS. Exposure to toxic agents: the heme biosynthetic pathway and hemoproteins as indicator. CRC Crit Rev Toxicol 1985;15:151-179.
3. Courtney KD. Hexachlorobenzene: a review. Environ Res 1979; 20:225-266.
4. Hahn ME, Gasiewicz TA, Linko P, Goldstein JA. The role of the Ah locus in hexachlorobenzene-induced porphyria: studies in congenic C57BL/6J mice. Biochem J 1988;254:245-254.
5. Jacobs JM, Sinclair PR, Bement WJ, Lambrecht RW, Sinclair JF, Goldstein JA. Oxidation of uroporphyrinogen by methylcholantrene-induced cytochrome P-450: essential role of cytochrome P-450d. Biochem J 1989;258:247-253.
6. Khanna RN, Smith AG. Fate of hexachlorobenzene in C57BL/10 mice with iron overload. Biochem Pharmacol 1985;34:4157-4162.
7. Stewart FP, Smith AG. Metabolism of the "mixed" cytochrome P450 inducer hexachlorobenzene by rat liver microsomes. Biochem Pharmacol 1986;35:2163-2170.
8. Sinclair PR, Bement WJ, Bonkovsky HL, Lambrecht RW, Frezza JE, Sinclair JF, Uruquhart AJ, et al. Uroporphyrin accumulation produced by halogenated biphenyls in chick-embryo hepatocytes. Biochem J 1986;237:63-71.
9. Ferioli A, Harvey C, De Matteis F. Drug-induced accumulation of uroporphyrin in chicken hepatocyte cultures: structural requirements for the effect and role of exogeneous iron. Biochem J 1984;224:769-777.
10. Sweeney G, Basford D, Rowley B, Goddard G. Mechanisms underlying the hepatotoxicity of 2,3,7,8-tetrachlorodebenzo-p-dioxin. Banbury Rep 1984;18:225-237.
11. Sinclair P, Lambrecht R, Sinclair J. Evidence for cytochrome P450-mediated oxidation of uroporphyrinogen by cell-free liver extracts from chick embryos treated with 3-methylcholantrene. Biochem Biophys Res Commun 1987;146:1324-1329.
12. Smith AG, Francis J. Chemically-induced formation of an inhibitor of hepatic uroporphyrinogen decarboxylase in inbred mice with iron overload. Biochem J 1987;246:221-226.
13. De Matteis F, Harvey C, Reed C, Hempenius R. Increased oxidation of uroporphyrinogen by an inducible liver microsomal system. Biochem J 1988;250:161-169.
14. Francis J, Smith AG. Oxidation of uroporphyrinogens by hydroxyl radicals: evidence for nonporphyrin products as potential inhibitors of uroporphyrinogen decarboxylase. FEBS Lett 1988;233: 311-314.
15. Rios de Molina MDC, Wainstock de Calmanovici R, San Martin de Viale LC. Investigations on the presence of porphyrinogen carboxy-lyase inhibitor in the liver of rats intoxicated with hexachlorobenzene. Int J Biochem 1980;12:1027-1032.
16. Cantoni L, Dal Fiume D, Rizzardini M, Ruggieri R. *In vitro* inhibitory effect on porphyrinogen carboxylyase of liver extracts from TCDD treated mice. Toxicol Lett 1984;20:211-217.
17. Elder GH, Tovey JA, Sheppard DM. Purification of uroporphyrinogen decarboxylase from human erythrocytes. Biochem J 1983;215:45-55.
18. De Matteis F. Role of iron in the hydrogen peroxide–dependent oxidation of hexahydroporphyrins (porphyrinogens): a possible mechanism for the exacerbation by iron of hepatic uroporphyria. Mol Pharmacol 1988;33:463-469.
19. Taljaard JJF, Shanley BC, Deppe WM, Joubert SM. Porphyrin metabolism in experimental hepatic siderosis in the rat. II. Combined effect of iron overload and hexachlorobenzene. Br J Haematol 1972;23:513-519.
20. Louw M, Neethling AC, Percy VA, Carstens M, Shanley BC. Effects of hexachlorobenzene feeding and iron overload on enzymes of haem biosynthesis and cytochrome P450 in rat liver. Clin Sci Mol Med 1977;53:111-115.
21. Sweeney GD, Jones KG, Cole FM, Basford D, Krestynski F. Iron deficiency prevents liver toxicity of 2,3,7,8-tetrachlorodibenzo-p-dioxin. Science 1979;204:332-335.
22. Blekkenhorst GH, Day RS, Eales L. The effect of bleeding and iron administration on the development of hexachlorobenzene-induced rat porphyria. Int J Biochem 1980;12:1013-1017.
23. Smith AG, Francis JE. Synergism of iron and hexachlorobenzene inhibits hepatic uroporphyrinogen decarboxylase in inbred mice. Biochem J 1983;214:909-913.
24. Alleman MA, Koster JF, Wilson JHP, Edixhoven-Bosdijk A, Slee RG, Kroos MJ, van Eijk HG. The involvement of iron and lipid peroxidation in the pathogenesis of HCB induced porphyria. Biochem Pharmacol 1985;34:161-166.
25. Wainstok de Calmanovici R, Billi SC, Aldonatti CA, San Martin de Viale LC. Effect of desferrioxamine on the development of hexachlorobenzene-induced porphyria. Biochem Pharmacol 1986; 35:2399-2405.
26. Aust SD, Svingen BA. The role of iron in enzymatic lipid peroxidation. In: Pryor WA, ed. Free radicals in biology, Vol V. New York: Academic Press, 1982:1-28.
27. Halliwel B, Gutteridge JMC. The importance of free radicals and catalytic metal ions in human diseases. Mol Aspects Med 1985;8: 89-193.
28. Visser O, van den Berg JWO, Edixhoven-Bosdijk A, Koole-Lesuis R, Rietveld T, Wilson JHP. Development of hexachlorobenzene prophyria in rats: time sequence and relationship with lipid peroxidation. Food Chem Toxicol 1989;27:317-321.
29. Waldo ED, Tobias H. Needle-like cytoplasmic inclusions in the liver in porphyria cutanea tarda. Arch Pathol 1973;96: 368-371.
30. Timme AH, Dowdle EB, Eales L. Symptomatic porphyria. Part I. The pathology of the liver in human symptomatic porphyria. S Afr Med J 1974;48:1803-1807.
31. Kosaka Y, Hagiwara M, Akeda S, Tameda Y, Tsujita E, Okuda Y, Shiomi Y, et al. Porphyria cutanea tarda with special reference to ultrastructural findings of the liver. Jpn J Gastroenterol 1981; 78:1635-1643.
32. James KR, Cortés JM, Paradinas FJ. Demonstration of intracytoplasmic needle-like inclusions in hepatocytes of patients with porphyria cutanea tarda. J Clin Pathol 1980;33:899-900.
33. Cortés JM, Oliva H, Paradinas FJ, Hernandez-Guio C. The

pathology of the liver in porphyria cutanea tarda. Histopathology 1980;4:471-485.
34. Kemmer C, Riedel H, Köstler E, Pätzold K. Zur Bedeutung parakristalliner Nadelstrukturen für die Diagnose der chronischen hepatischen Porphyrie- licht und elektronenmikroskopische Untersuchungen an Biopsiematerial. Zentralbl Allg Pathol 1983;127:253-264.
35. Chlumska A, Chlumsky J, Krtek V, Malina L. Crystalline inclusions in hepatocytes in patients with late cutaneous porphyria [in Czech]. Vnitr Lek 1981;27:1110-1113.
36. Ostowski J, Michalak T, Zawirska B, Kostrzewska E, Blaszczyk M, Gregor A. The function and morphology of the liver in porphyria cutanea tarda. Ann Clin Res 1984;16:195-200.
37. Fakan F, Chlumska A. Demonstration of needle-like inclusions in porphyria cutanea tarda using the ferric ferricyanide reduction test. Virchows Arch [A] 1987;411:365-368.
38. Medline A, Bain E, Menon AI, Haberman HF. Hexachlorobenzene and rat liver. Arch Pathol 1973;96:61-65.
39. Timme AH, Taljaard JJF, Shanley BC, Joubert SM. Symptomatic porphyria. Part II. Hepatic changes with hexachlorobenzene. S Afr Med J 1974;48:1833-1836.
40. Mollenhauer MH, Johnson JH, Younger RL, Clark DE. Ultrastructural changes in liver of the rat fed hexachlorobenzene. Am J Vet Res 1975;36:1777-1781.
41. Böger A, Koss G, Koransky W, Naumann R, Frenzel H. Rat liver alternations after chronic treatment with hexachlorobenzene. Virchows Arch [Pathol Anat] 1979;382:127-137.
42. Petryka ZJ, Kostich ND, Dhar GJ. Location of iron and porphyrin in the liver in porphyria cutanea tarda. Acta Histochem (Jena) 1978;63;168-176.
43. Wilson JHP, van den Berg JWO, Edixhoven-Bosdijk A, van den Gastel-Quist LHM. Preparation of porphyrin methylesters for high pressure liquid chromatography. Clin Chim Acta 1978;89: 165-167.
44. Lowry OH, Rosebrough NJ, Farr AL, Randall RJ. Protein measurement with the folin-phenol reagent. J Biol Chem 1951; 193:265-275.
45. Francis JE, Smith AG. Assay of mouse liver uroporphyrinogen decarboxylase by reverse-phase high-performance liquid chromatography. Anal Biochem 1984:138:404-410.
46. Harris DC. Iron exchange between ferritin and transferrin *in vitro*. Biochemistry 1978;17:3071-3078.
47. Lillie RD, Fullmer HM. Histopathologic technic and practical histochemistry. 4th ed. New York: McGraw-Hill, Inc., 1976:235-238;507-508.
48. Sorber CWJ, de Jong AAW, den Breejen NJ, de Bruijn WC. Quantitative energy-filtered image analysis in cytochemistry. I. Morphometric analysis of contrast-related images. Ultramicroscopy 1990;32:55-68.
49. Sorber CWJ, van Dort JB, Ringeling PC, Cleton-Soeteman MI, de Bruijn WC. Quantitative energy-filtered image analysis in cytochemistry. II. Morphometric analysis of element-distribution images. Ultramicroscopy 1990;32:69-79.
50. Cleton MI, Mostert LJ, Sorber LWJ, de Jong AAW, de Jeu-Jaspars CMH, de Bruijn WC. Effect of phlebotomy on the ferritin iron content in the rat liver as determined morphometrically with the use of electron energy loss spectroscopy. Cell Tissue Res 1989; 256:601-605.
51. Ploem JS. Reflection contrast microscopy as a tool for investigation of the attachment of living cells to a glass surface. In: van Furth R, ed. Mononuclear phagocytes in immunity, infection and pathology. Oxford: Blackwell, 1975:405-421.
52. Cornelese-ten Velde I, Prins FA. New sensitive light microscopical detection of colloidal gold on ultrathin sections by RCM: combination of reflection contrast and electron microscopy in post-embedding immunogold histochemistry. Histochemistry 1990;94: 61-71.
53. Cleton MI, Frenkel EJ, de Bruijn WC, Marx JJM. Determination of iron to phosphorus ratios of iron storage compounds in patients with iron overload: a chemical and electron probe x-ray microanalysis. HEPATOLOGY 1986;6:848-851.
54. Lillie RD, Donaldson PT. The mechanism of the ferric ferricyanide reduction reaction. Histochem J 1974;6:679-684.
55. Smith AG, Francis JE, Cabral JRP, Carthew P, Manson NM, Stewart FP. Iron-enhancement of the hepatic porphyria and cancer induced by environmental polyhalogenated aromatic chemicals. In: Poli G, Cheeseman KH, Dianzani MU, Slater TF, eds. Free radicals in the pathogenesis of liver injury, adv bioscien. Vol. 76. Oxford: Pergamon Press, 1989:203-214.
56. Smith AG, De Matteis F. Oxidative injury mediated by the hepatic cytochrome P-450 system in conjunction with cellular iron: effects on the pathway of haem biosynthesis. Xenobiotica 1990;20: 865-877.
57. Van Wyk CP, Linder-Horowitz M, Munro HN. Effect of iron loading on non-heme iron compounds in different liver cell populations. J Biol Chem 1971;246:1025-1031.
58. Greig JB, Francis JE, Kay SJE, Lovell DP, Smith AG. Incomplete correlation of 2,3,7,8-tetrachlorodibenzo-p-dioxin hepatotoxicity with Ah phenotype in mice. Toxicol Appl Pharmacol 1984;74: 17-25.
59. Cheeseman KH, Proudfoot KA, Maddix SP, Collins MM, Milia A, Slater TF. Low rate of NADPH/ADP-iron dependent lipid peroxidation in hepatic microsomes of DBA/2 mice. FEBS Lett 1985; 184:343-346.
60. Smith AG, Francis JE, Dinsdale D, Manson MM, Cabral JRP. Hepatocarcinogenicity of hexachlorobenzene in rats and the sex difference in hepatic iron status and development of porphyria. Carcinogenesis 1985;6:631-636.
61. Munro HN, Linder MC. Cells sequence Fe^{2+} in ferrules. Physiol Rev 1978;58:317-396.
62. De Matteis F, Stonard M. Experimental porphyrias as models for human hepatic porphyrias. Semin Hematol 1977;14:187-192.
63. Rowley B, Sweeney GD. Release of ferrous iron from ferritin by liver microsomes: a possible role in the toxicity of 2,3,7,8-tetrachlorodibenzo-p-dioxin. Can J Biochem Cell Biol 1984;62: 1293-1300.
64. Jacobs A. Low molecular weight intracellular iron transport compounds. Blood 1977;50:433-439.
65. Wills ED. Lipid peroxide formation in microsomes: the role of non-haem iron. Biochem J 1969;113:325-332.
66. Bakkeren DL, de Jeu-Jaspars CHM, van der Heul C, van Eijk HG. Analysis of iron-containing components in the low molecular weight fraction of rat reticulocyte cytosol. Int J Biochem 1985; 17:925-930.
67. Mukerji SK, Pimstone NR, Burns M. Dual mechanism of inhibition of rat liver uroporphyrinogen decarboxylase activity by ferrous iron: its potential role in the genesis of porphyria cutanea tarda. Gastroenterology 1984;87:1248-1254.